Flow Visualization in engraved champagne tasting glasses

Fabien Beaumont [1,*], Gérard Liger-Belair [2], Guillaume Polidori [1]

[1] GRESPI/Thermomécanique, EA4301
[2] GSMA/Equipe Effervescence, Champagne et Applications, UMR CNRS 7331
Faculty of Science, University of Reims, France
*corresponding author: fabien.beaumont@univ-reims.fr

Abstract: Glass shape and especially his open aperture is suspected to play an important role as concerns the kinetics of CO_2 and flavor release during champagne tasting. In recent years, much interest has been devoted to depict each and every parameter involved in the release of gaseous CO_2 from glasses poured with champagne. One cannot understand the bubbling and aromatic exhalation events in champagne tasting, however, without studying the flow-mixing mechanisms inside the glass. Indeed, a key assumption is that a link of causality may exist between flow structures created in the wine due to bubble motion and the process of flavor exhalation. In this article, a collection of various ascending bubble driven flow patterns and mixing phenomena, which illustrate the fine interplay between ascending bubbles and the fluid around, were evidenced, through tomography techniques. Moreover, the Particle Image Velocimetry (PIV) technique was used in order to reach the velocity field of the ascending bubbles-driven flow patterns found in a flute poured with champagne. The results show that the continuous flow of ascending bubbles strongly modifies the mixing and convection conditions of the liquid medium. Moreover, spontaneous and self-organized convective cells were evidenced at the air/champagne interface through laser tomography. The number, size and velocity of the multiple and self-organized convective cells vary as time proceeds with the continuously decreasing bubble driven champagne flow. We can establish a close link between the number of hydrodynamic instabilities evidenced at the air/champagne interface and the bubble flow rate.
Keywords: Champagne, laser tomography, PIV, flows topology, vortex flow, two-phase flow.

1 Introduction

Associated with luxury and celebrations, champagne is elaborated according to the "méthode traditionnelle". The progressive release of gaseous CO_2 from the liquid medium is responsible for bubble formation (the so-called effervescence process). From the consumer point of view, the role of bubbling is essential in champagne. A key assumption in the champagne tasting analysis is that a link of causality is suspected between effervescence and the high olfactory and gustatory levels of this French sparkling wine. Moreover, the role of effervescence is suspected to go far beyond the solely aesthetical point of view. It was indeed recently demonstrated that the continuous flow of ascending bubbles strongly modifies the mixing and convection conditions of the liquid medium. In turn, the CO_2 discharge by diffusion through the free air/champagne interface may be considerably accelerated, as well as the release of the numerous volatile (and potentially aromatic) organic compounds (VOC) which both strongly depend on the mixing flow conditions of the liquid medium. For all the aforementioned reasons, a very strong coupling was therefore suspected in champagne tasting, between dissolved CO_2, the presence of rising bubbles, glass shape, CO_2 discharge and VOC release. Quite recently, much attention has been paid by glassmakers and champagne houses to eventually better control the kinetics of bubble nucleation and effervescence in champagne glasses [1-2].

This study is based on the idea that one cannot be interested in the CO_2 discharge and VOC release without showing interest to the bubbles driven flow patterns and mixing phenomena. A perfect knowledge of the laws governing the fluid flows seems unquestionably the best way to control the release of gaseous CO_2 all along tasting.

2 Bubble driven flow patterns

In a glass of champagne, the bubble driven flow patterns are invisible to the naked eye. Our visualization is based on a laser tomography technique, where a 2 millimeters wide laser sheet crosses the center line of the flute, imaging just this two-dimensional section of the glass. The laser tomography technique revealed the flow

structure which strongly depends on the effervescence intensity but also of the glass shape [2-4]. This technique, although qualitative, gives us valuable information about the mixing flow phenomena during a tasting. These convective movements actively participate in gaseous and aromatic exchanges between the liquid and the gaseous phases. The information obtained through the laser tomography will enable to access by indirect way to some topological data such as streaklines and streamlines.

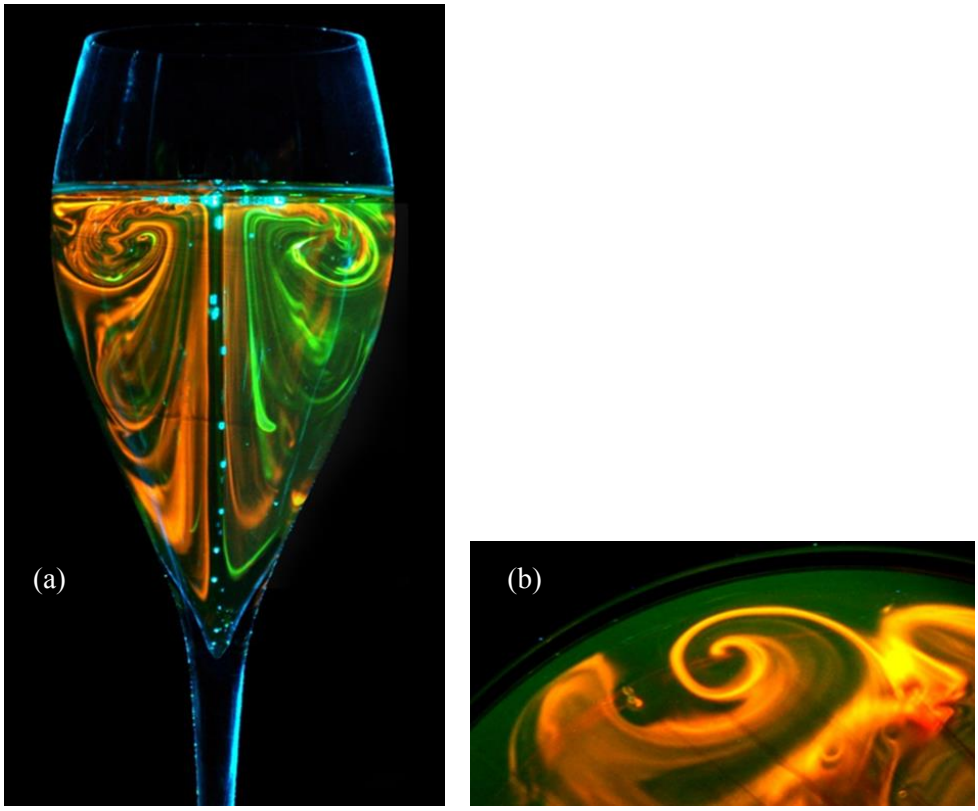

Figure 1: The laser tomography technique and the use of two different fluorescent dyes (fluorescein and sulforhodamine) allows to highlight the flow patterns in the plane of symmetry of a tulip-shape glass (a), swirling flow visualized by sulforhodamine injection to the liquid surface of a champagne coupe (b) [3-4].

a) Effervescence and convection

Consider the example of a bubble released from a nucleation site, a dust or a cellulose fiber for example. Owing to viscous effects, ascending bubbles create a field of adverse pressure in their near wakes. Consequently, champagne bubbles and the neighboring liquid rise as concurrent vertically oriented flows along the axis of symmetry of the glass. Because the bubble nucleation process from a given nucleation site is a clockwork repetitive process, the champagne bulk is therefore subjected to a continuous driving process. Very recently, it was indeed demonstrated that ascending bubbles act as so many swirling motion generators in champagne glasses. In the case of bubbles nucleated at the bottom of the glass and rising on the axis of symmetry, the resulting flow is axisymmetric, as illustrated in Figure 1 (a). During the filling process of the glass, Rilsan particles are added to the wine. These polymer particles are quasi-spherical in shape, with diameters ranging from 50 to 75 micrometers, and have a density (1.060) close to that of Champagne (0.998). The particles are neutrally buoyant and do not affect bubble production, but they are very reflective of laser light. Since the laser sheet cutting the glass in its symmetry plane, the liquid path may be revealed during the exposure time of a camera. Figure 2 (a) shows a bubble train nucleated from a cellulose fiber. Convective liquid movement are highlighted through continuous and discrete tracers made visible by laser tomography. Since the laser sheet passes through the plane of symmetry of the glass, the tracer trajectory is fixed during the exposure time of the camera (in general, 1 to 4 seconds). Thus, the use of discrete and continuous tracers allows us to deduce the steamlines and the streaklines presented in Figure 2 (b) and (c) for an isolated bubble train.

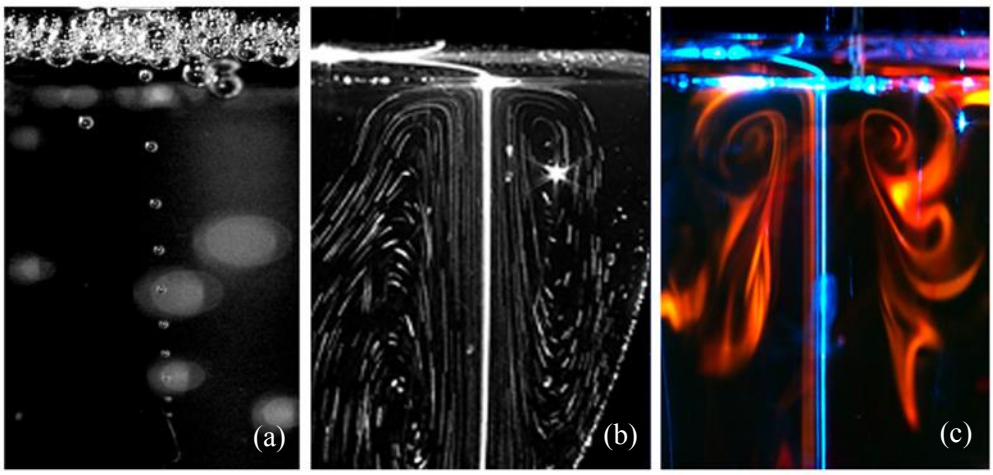

Figure 2: Bubbles train released from a cellulose fiber (a), streamlines (b) and streaklines (c) obtained through laser Tomography [1].

b) Natural and artificial nucleation

When several bubbles trains coexist simultaneously in a glass, the continuous flow of bubbles is able to put all the liquid in motion. To overcome a deficit of natural nucleation sites (dust, cellulose fibers ...) when the glass is washed in the dishwasher for example, glassmakers realize some scratches at the bottom of the glasses. These etchings, usually disposed in a ring, are carried out by laser impacts. The micro scratches generated around the laser impact can trap some air pockets during the pouring process, forcing the heterogeneous nucleation process of champagne bubbles. Figure 3 shows a tomography performed with solid tracers in an unetched flute (a) and in a flute mechanically engraved (b).

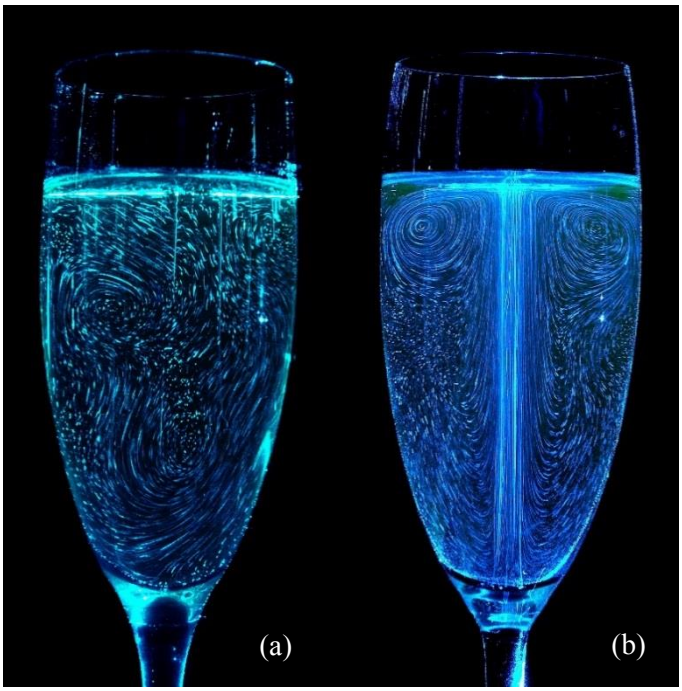

Figure 3: Flow Visualization in two glasses, one has a natural effervescence (a), the other is engraved (b) [1].

In the case of the etched flute, several tens of bubble trains, coming from the etching crown ensure uniform mixing of the liquid [5-6]. On the other hand, non-engraved flute shows a "natural" effervescence and perfectly

random in both the number of nucleation sites as their location on the glass walls [7]. In this case, the wine is agitated by swirling motions which allow a homogeneous and relatively slow liquid mixing. Because the gas column acts like a continuous swirling-motion generator within the glass, the flow exhibits a quasi-steady two-dimensional behaviour with an axis-symmetrical geometry (Figure 3 (b)). In the etched flute, the shape of the flow is different. In the laser plane, the main flow consists of two symmetrical vortices disposed on either side of the central column of bubbles. And since the bubbles train is located on the axis of symmetry of the glass, the resulting flow is axisymmetric. In the case of the etched flute, the wine is also stirred homogeneously, but the liquid phase velocities are higher than those measured in the unetched flute. Actually, because the flute exhibits cylindrical symmetry around its central axis, the real three-dimensional structure of the flow patterns in the bulk is that of a deformed torus. The way the liquid will be mixed will therefore depend on the amount of nucleation sites present in a glass. When the glass is etched, the number of laser beam impacts will influence the dynamics of the vortex flow.

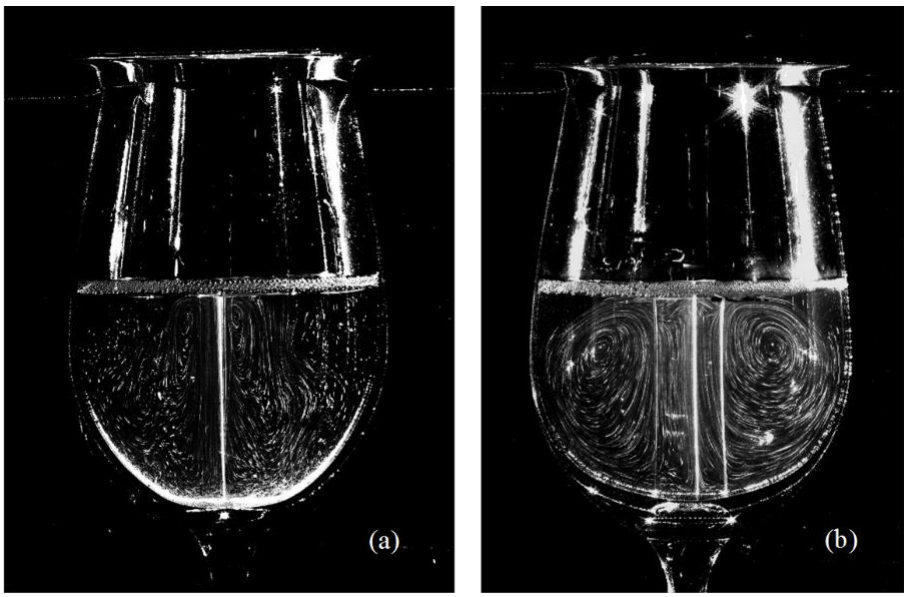

Figure 4: Flow visualization in an INAO etched glass, one having a single laser beam impact (a) and the other 50 laser beam impacts (b).

Figure 4 shows two tomographies performed in the same INAO glass, one having a single laser beam impact (a) and the other 50 laser beam impacts (b). Each bubble train is able to drain some liquid but a single bubble train does not allow to mix the whole of the liquid, the kinetic energy carried by the bubbles is not sufficient (Figure 4a). In contrast, 50 laser beam impacts disposed in a small ring allow the whole mixing of the wine. Therefore, at a given time, there will be a minimum number of laser beam impacts from which all the liquid will be mixed.

In a flute, with a narrow aperture (Figure 5 a), the vortex ring occupies all available space [3]. Because of its large filling height, the wine mixing intensity is high. Conversely, in the coupe (Figure 5 b), the low filling height does not allow to the bubbles to take enough velocity and the aperture is much wider than the flute. Consequently, the bubbles will not have sufficient kinetic energy to set in motion all the liquid. Moreover, in the coupe, the vortex ring will not occupy all available space. At the edge of the central zone mixed by the ascending bubbles, the coupe present some zones where the liquid is substantially inert. As time proceeds, the amount of dissolved carbon dioxide contained in the wine decreases [8-9]. This has the consequence of reducing the bubble size and the effervescence intensity. Thus, since the bubbles act as a motor for the main flow, we will find topological changes in the flow structure during a tasting.

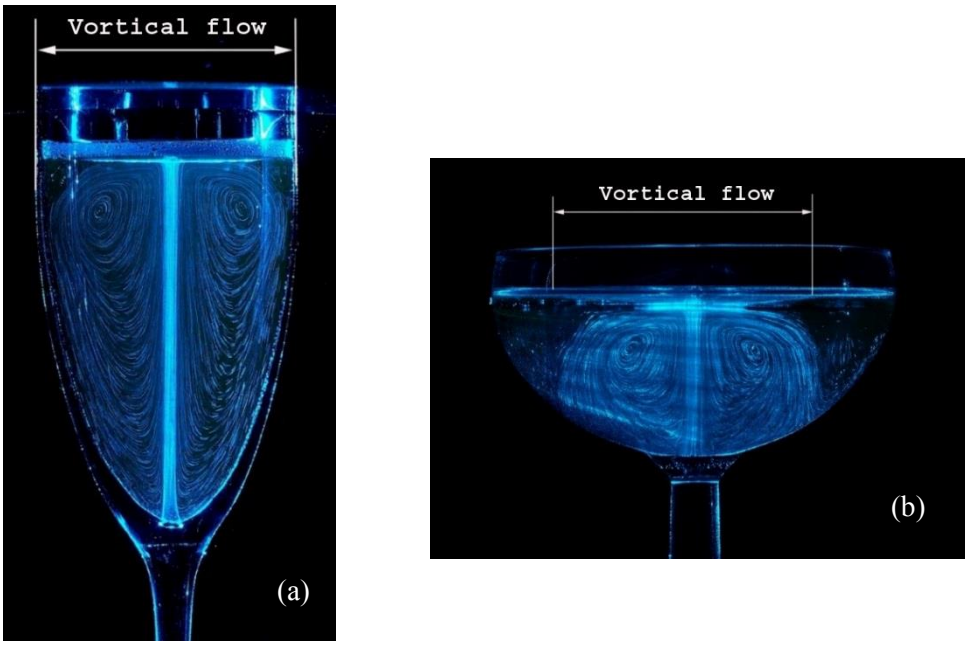

Figure 5: Flow visualization in two identically engraved glasses but with different forms: the flute (a) and the coupe (b).

c) Topological analysis method

The analysis method of topology of the average velocity field that we use consist in the identification and description of the critical points, called singular points, of the flow. Perry and Fairlie [10] introduced the theory of critical points and its application to fluid flow. This method has proved its efficiency (Hunt et al. [11] Perry and Chong [12-13]).

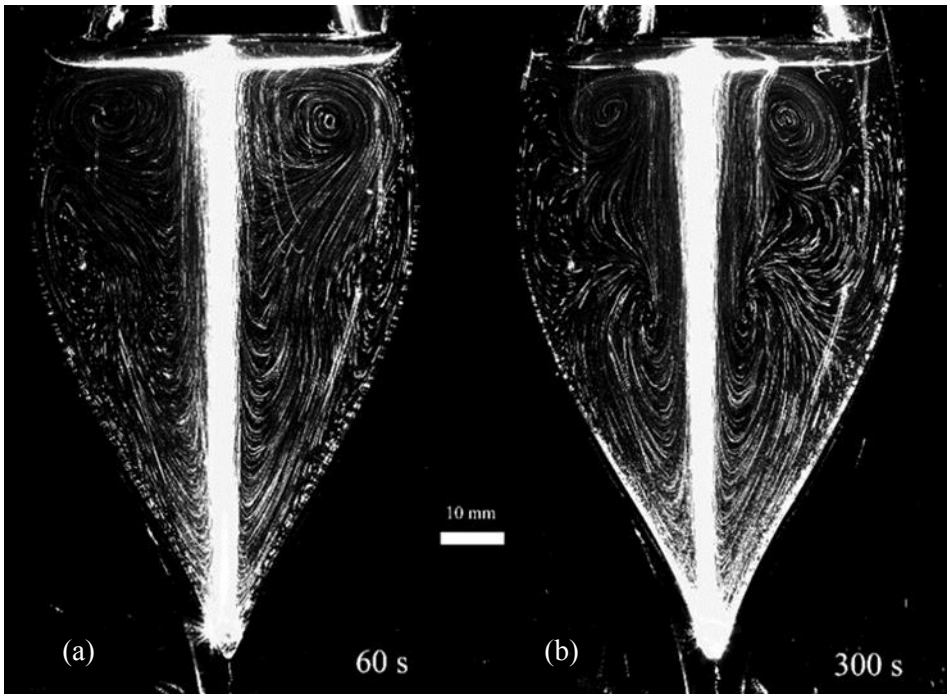

Figure 6: Flow visualization in the tulip flute 60 s (a) and 300 s after the filling process (b). Progressive topological modification of flow.

In our study, the flow structure, conditioned by the revolution symmetry of the glass is time dependent and varies throughout a tasting depending on the intensity of the effervescence [14-16].

Hunt et al. [11] showed that for a geometry such as ours:

$$\sum N - \sum S = -2 \quad (1)$$

Where ΣN represents the sum of nodes (including spirals and centers) and half-nodes, and ΣS the sum of the saddles and half saddles.

This means that, according to equation (1), in order to reach the topological equilibrium, it is necessary that the sum of the half-nodes and nodes subtracted from the sum of the saddles and half-saddles have to be equal to -2.

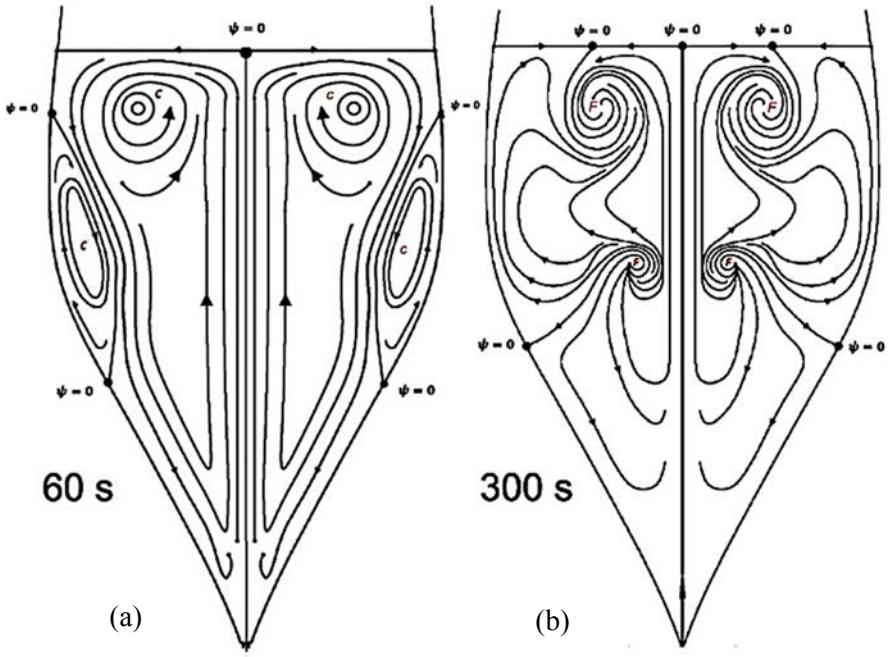

Figure 7: Streamlines deduced from figure 6 in the tulip-shaped glass at t=60 s (a) and t=300 s after the pouring process (b).

Then we can use the term "topological equilibrium" for a flow such that the theorem Hunt (1) is verified. In practice, we have plotted the streamlines from the tomographies shown in Figure 6.

The streamlines represented on the Figure 7 allow to describe the topology of the flow for two moments after the pouring process (one and five minutes). Based on the streamlines, we identify the type of critical points.

Thus, we can consider the structure of the flow for two times t = 60 sec and t = 300 sec:

At t = 60 s, N = 4 centers and S = 6 saddles.

At t = 300 s, N = 4 spirals and S = 6 saddles.

One minute after the pouring process, the sum of nodes (including spirals and centers) and half-nodes are equal to 4. The sum of the saddles and half-saddles S is equal to 6. Five minutes after the pouring process, the sum of nodes (including spirals and centers) and half-nodes are equal to 4. The sum of saddles and half-saddles S is equal to 6.

The results show us that the topological equilibrium is observed whatever the time following the pouring process.

3 PIV measurements of the flow dynamic

Until now, the results presented in this paper have shown the unsteady evolution of the flow topology during a champagne tasting. We will now interested in the dynamics of convection movements induced by the bubbles in a glass of champagne [17]. These results, complementary to the precedent work done with laser tomography techniques are performed to compare the dynamics of the mixing processes whatever the shape of the glass. We believe that there is a correlation between the velocities of the convection movements in a supersaturated liquid (carbon dioxide), the diffusion velocity of this gas at the surface and the release of volatile organic molecules. Measurements have been carried out in order to quantify the velocities of convective mixing process during a tasting.

PIV Experimental setup

The experimental configuration of the PIV measurement system includes a LITRON Nd: YAG laser emitting at 532 nm with a maximum power of 135 mJ. The laser sheet is created throughout a cylindrical lens. Image acquisition is done by a CCD camera, Flow sense model, which is able to record 14-bit black and white images. The duration of a laser pulse is 250 ms and the acquisition frequency is 4 Hz. Images acquisition is performed in double frame mode by a sequence of 50 images. The averaged correlation is used as the analysis method. This method can reproduce a vector field from several pairs of images by determining the average correlation in an interrogation zone. The glass is set in a tank filled with water in order to avoid optical distortion due to the shape of the glass. Champagne (or sparkling wine) is a wine where two phases coexist (a gaseous and a liquid phase), it's a two-phase flow.

In order the bubbles are not considered as tracers by the PIV system, we have disposed an interference filter before the lens of the camera. At the time of pouring process, the wine, previously poured into the glass, is seeded with rhodamine B particles. When the flow is excited by the laser, the filter lets through only the wavelengths re-emitted by the rhodamine particles. The measurements were performed under the same experimental conditions than for laser tomography experiments. A bottle of champagne is opened for each new experiment in order to have substantially the same initial rate of dissolved carbon dioxide. Because the flow in a champagne glass is biphasic, with the co-presence of a liquid phase and a gaseous phase, an interference filter is placed before the camera to subtract the bubbles to the recorded images. The wine, previously poured into the glass, is seeded with rhodamine B particles at the time of pouring process. Measurements are performed at the temperature of the experimental room: 20 ± 0.5 ° C. Some sequences of 20 images are recorded at different times following the pouring process in order to monitor the flow dynamics according to time. The average correlation is used as an analytical method. The resulting velocity vectors are used to deduce information such as the streamlines, the velocity profiles or the velocity isocontours.

a) Flow topology

Figure 8 shows the streamlines of the liquid phase deduced by PIV in a coupe filled with 100 ml of champagne for 3 minutes following the pouring process. Figure 9 represents the flow topology at t = 2 minutes after the pouring process. At this time, all the wine is mixed and the flow consists of a main vortex structure named $T1$ that occupies about 2/3 of the available space. Two co-rotating vortex cells named $T2$ and $T3$, smaller than $T1$, and with c2 and c3 centers, rotate in opposite direction regarding to the main vortex ring. We can also notice the beginnings of a spiral named $F1$ and located along the glass wall. 5 minutes after the pouring process, the size of the vortex ring $T1$ has decreased. The second co-rotating cell $T3$ have merged with the swirling cell $T2$. Ten minutes after the pouring process, the mixed liquid volume still decreases and the heart $C1$ of the main vortex ring $T1$ is close to the axis of symmetry of the glass (Figure 8). There remains only one vortex cell $T2$ which rotate in opposite direction of the main flow.

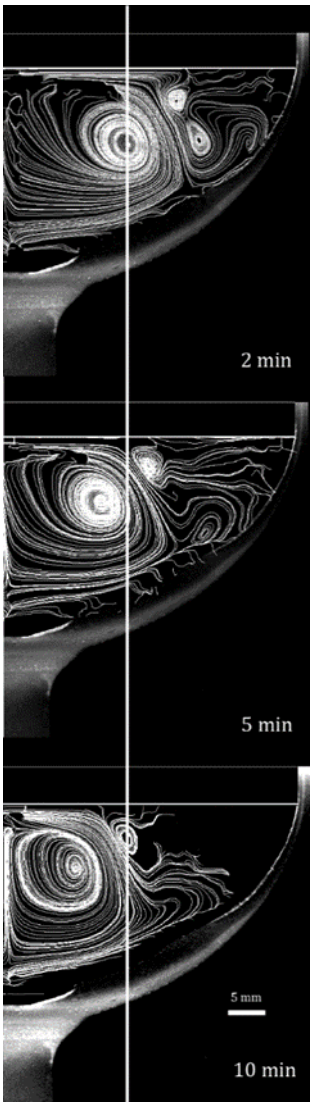

Figure 8: Streamlines of the liquid phase for 3 moments after the pouring process, the white line is used to monitor the position of the heart of the main flow vortex.

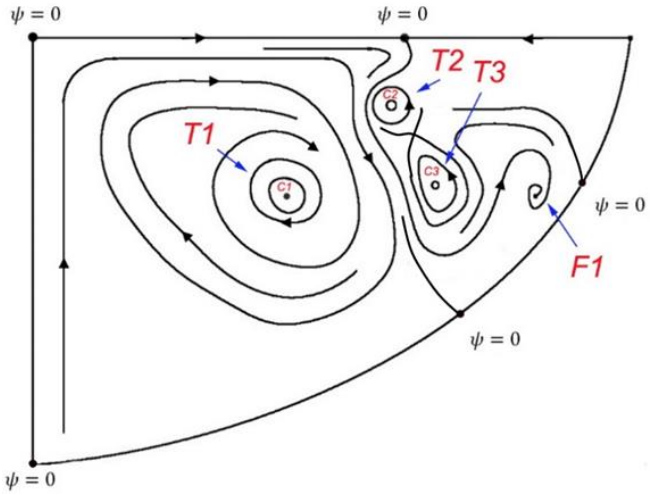

Figure 9: topological diagram of the flow in a half of the coupe deduced from the figure 8 for 2 minutes after the pouring process.

b) Coalescence of corotating vortices

The flow is complex, but anyway, the vortex flow structure following topological rules already studied in the literature. We refer to the article by Badr et al. [18] in which the authors propose a scheme on the coalescence of two co-rotating eddies. We start from the streamlines at t=2 minutes, corresponding to the time t1 to explain the coalescence of two vortices.

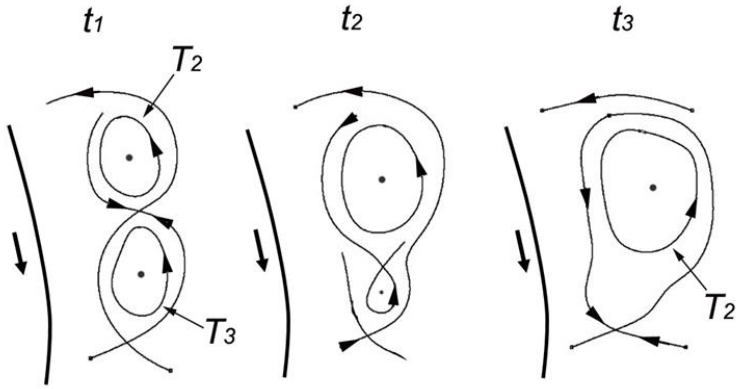

Figure 10: Coalescence of two vortices, according Badr et al. [18].

Figure 10 shows the coalescence of two vortices. At time t1, we have two separate vortices T2 and T3, each with its own center and its own saddle. At time t2, and because their size has changed over time, they come into contact with each other, leading to a 8-shaped structure around the 2 centers. In this configuration, we have two saddles and two centers. Progressively, the vortex T2 continuously grows up until completely absorb the vortex T3 at time t3 to form one single vortex.

c) Velocity profiles

After the pouring process, the progressive decrease of dissolved carbon dioxide rate causes a decrease in the velocity of the bubbles. Thus, as the bubbles set in motion the liquid and that their velocity decreases over time, the dynamics of the wine mixing is progressively modified. The laser tomography and the PIV showed us the existence of topological changes in the flow during a tasting. In order to investigate the unsteady dynamic of the liquid phase, we achieved PIV measurements of the liquid phase velocities in the tulip glass-shape during the 10 minutes after the pouring process. Some sequences of 20 images were recorded at different intervals. Fields vectors, corresponding to 2, 5 and 10 minutes after the pouring process, were deduced from an average correlation. From these vector fields, we were able to extract some velocities profiles showing the evolution of the dynamics of the mixing processes in a champagne glass over time.

Figure 12 represents the mean velocity profiles plotted along a horizontal axis passing through the heart of the main vortex flow (Figure 11) and for 3 moments after the pouring process (2, 5 and 10 minutes). The results show a gradual decrease in velocities of the liquid phase over time. The highest velocities, of about 9 cm / s, are located at the center of the glass, in the wake of the bubbles. We can also observe a decreasing evolution of the vortex intensity.

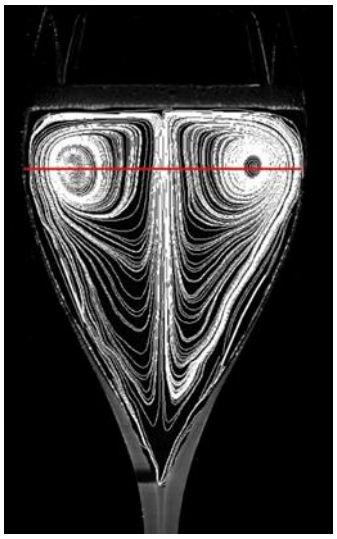

Figure 11: streamlines of the liquid phase obtained by PIV in the tulip glass-shape 3 minutes after the pouring process. The red line represents the horizontal axis along which we plotted the velocity profiles.

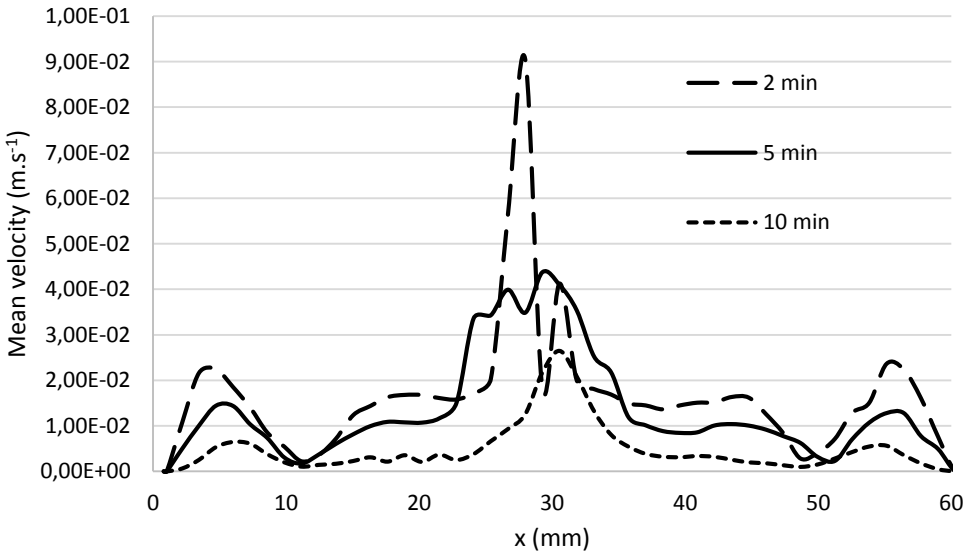

Figure 12: Mean velocity of the liquid phase plotted along a horizontal axis passing through the vortex cores.

4 hydrodynamic instabilities found at the liquid / air interface

a) Laser Tomography

Laser tomography and particle image velocimetry (PIV) techniques were used in order to explore the flow patterns found at the air/champagne interface [19-20]. The laser sheet (previously vertically oriented in order to investigate the flow patterns found within the champagne bulk) was positioned parallel to the champagne surface, with a grazing incidence with regard to the air/champagne interface. The air/champagne interface was also seeded with Rilsan particles in order to make visible the two-dimensional (2D) flow patterns through laser tomography. Nevertheless, it is worth noting that champagne bubbles floating at the liquid surface may also intercept the laser sheet. Floating bubbles, which freely follow the 2D movement of the air/champagne interface (exactly as drifting buoys do to track sea surface currents), therefore contribute to track the trajectories of champagne surface currents. A collection of multiple 2D vortices self-organized at the

air/champagne interface, as evidenced through laser tomography, is displayed in Figure 13. Those vortices are the result of the fine interplay between ascending bubbles which continuously drive some fluid parallel to the champagne surface (as bubbles reach the interfacial boundary layer) and the circular glass edge, which confines the surface fluid circulation around its boundary.

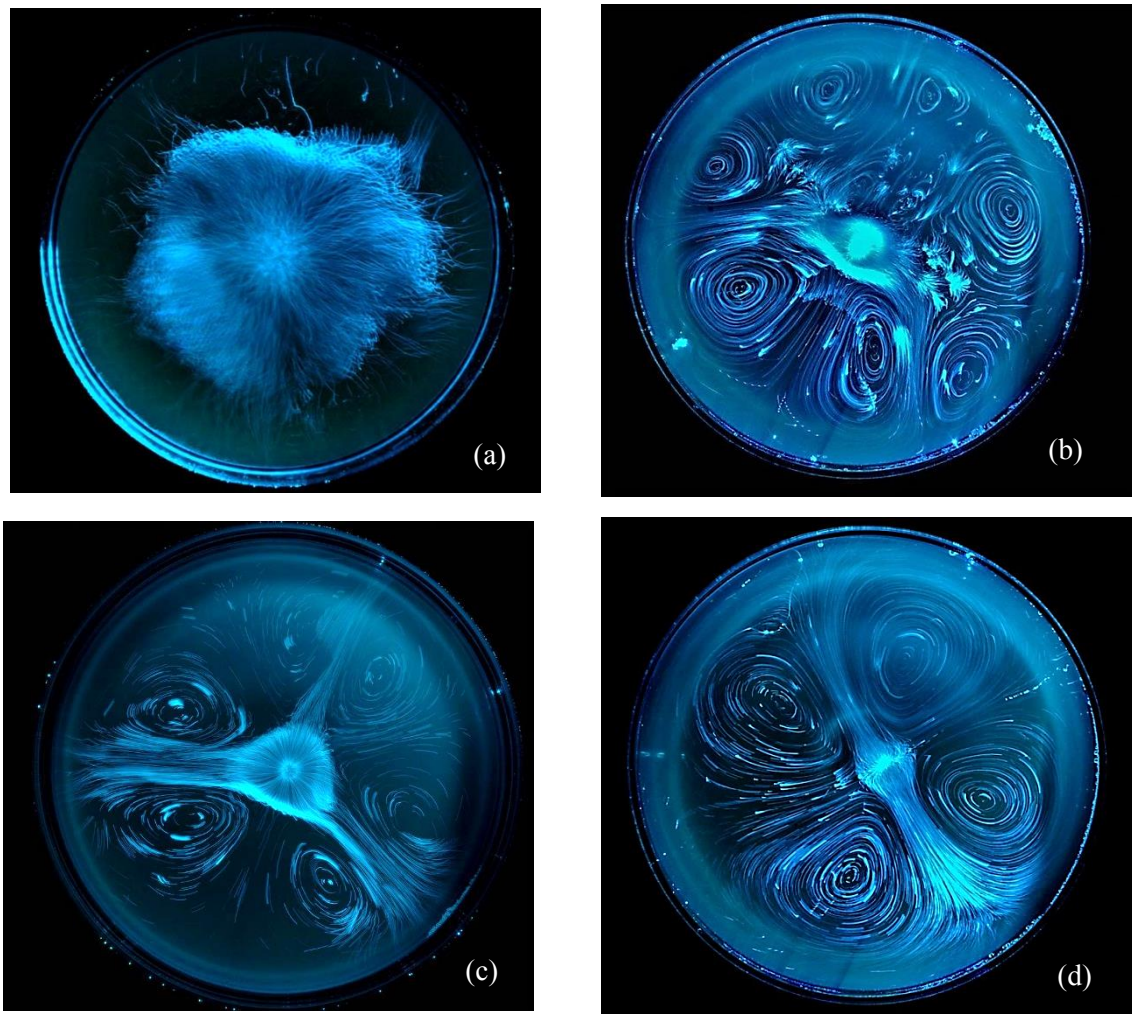

Figure 13: spontaneous self-organised 2D convective cells at the surface of a coupe filled with champagne (and with a laser etched circular pattern which generates a constant stream of bubbles from its bottom), as unravelled through laser tomography: the number, size and velocity of the multiple and self-organised convective cells may nevertheless vary as time proceeds with the continuously decreasing bubble driven champagne flow.

The number of counter-rotative cells may vary as time proceeds, but the most usual surface structure is a four counter-rotative convective cells structure (as the last two frames displayed in Figure 13).

The results of these tomographies show that the number of counter-rotating cells varies depending on the time elapsed since the pouring process. However, we can define a "stable" mode, corresponding to the presence of four counter-rotating cells disposed around the central axis of the glass. This mode is consistently observed a few minutes after the pouring process. The first mode, observed just after the pouring process is a highly unstable mode (a).

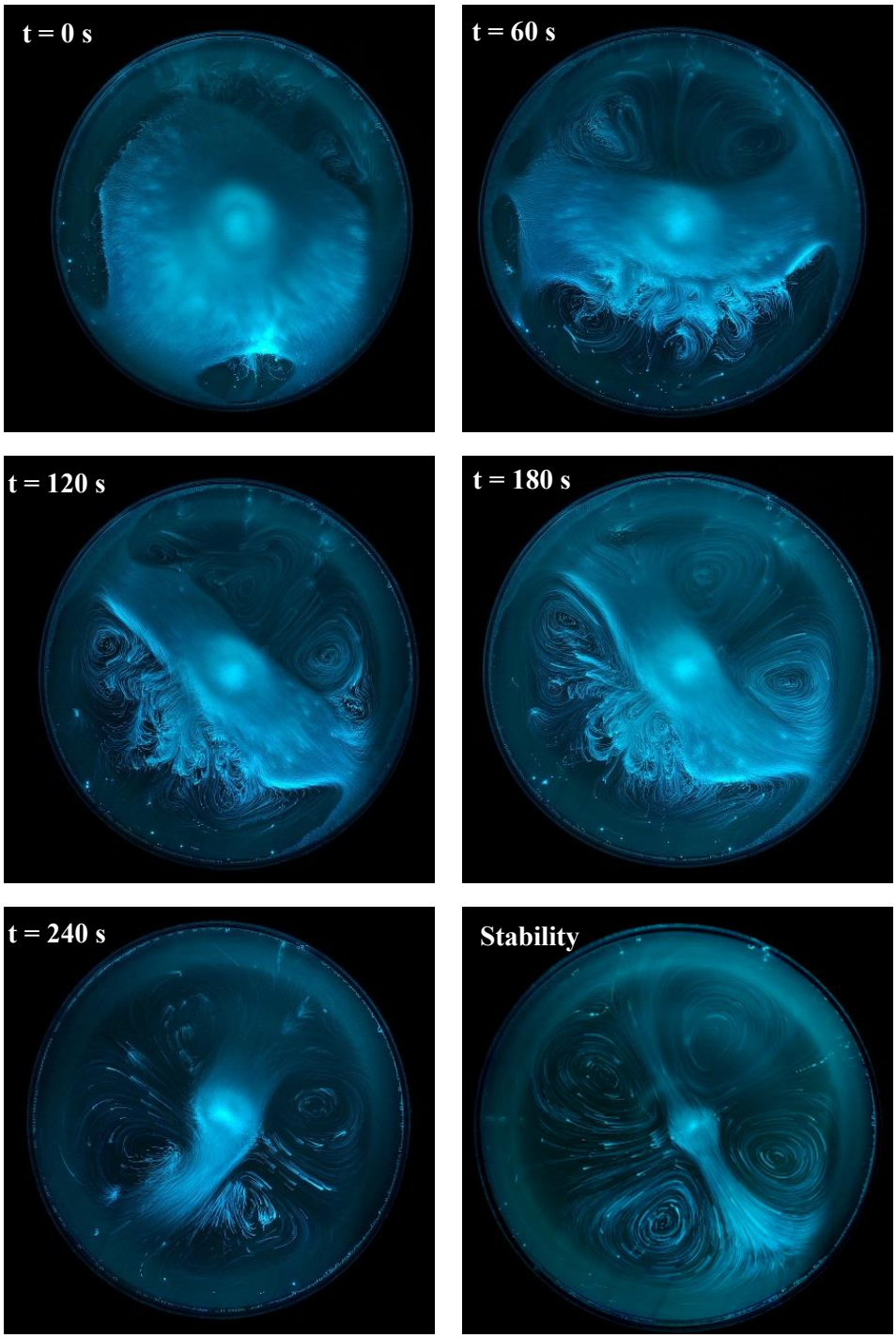

Figure 14: Development chronology of surface vortex cells.

The second mode, observed a few seconds after the pouring process is an unsteady mode composed of many cells, this mode is constantly evolving with time (b). The third mode corresponds to the presence of 6 cells disposed around three principal axes (c). The fourth and final mode is a stable mode composed of four counter-rotating cells disposed around two main axes (d). This stable mode appears a few minutes after the pouring process.

Since the vortex cells vary in degressive number after the pouring process, we think that there is a strong relationship between the velocity of the flow patterns induced by the bubbles and the number of instabilities observed on the surface. The number of cells varies according to the intensity of the bubbles flow rate. We noticed that when the bubble flux is still very intense (the first moments after the pouring process), the number of vortices is very unstable (Figure 13 (b)) and seems to hesitate between four, six or eight cells. At the liquid

surface, the vortices can merge with each other or be divided into two new vortices. Figure 14 indicates the formation sequence of convective cells. However, regardless of the intensity of the effervescence, we find an unsteady mode, with the presence of multiple cells and a stable mode, which occurs within minutes after the pouring process. The flow organizes itself and direction of the feed streams is established according to the preferred or flow axe directions. We will call flow axes, the feed stream of hydrodynamic instabilities which ensures the circulation of liquid in only one component x, y or z. In this sequence, only two flow axes are visible. We can also establish a link between the number of flow axes and the number of convective cells since two axes will give four vortex cells, 3 axes, six vortex cells and so on...

Laser tomography allows visualization of a slice of flow in a 2D plane. However, we believe there is a strong coupling between the flows observed in the liquid matrix and those highlighted in air / wine interface (Figure 15).

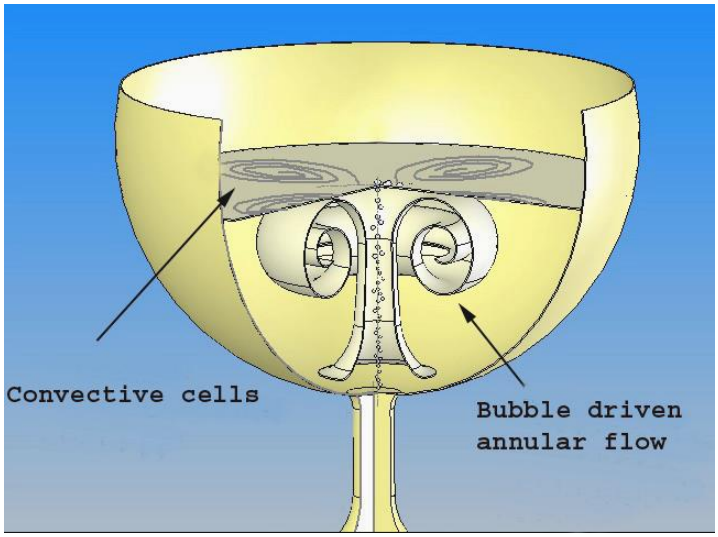

Figure 15: 3D Illustration of the fluid flow patterns in a champagne glass.

Figure 16 (a) shows the detail of a vortex cell resulting from a laser tomography. Swirling, fluid dives into the liquid matrix, reinforcing the idea that the flow is three-dimensional. In this configuration, the vortex takes a helical shape (Figure 16 (b)). We believe these convective cells develop in a layer of several millimeters under the air / liquid interface.

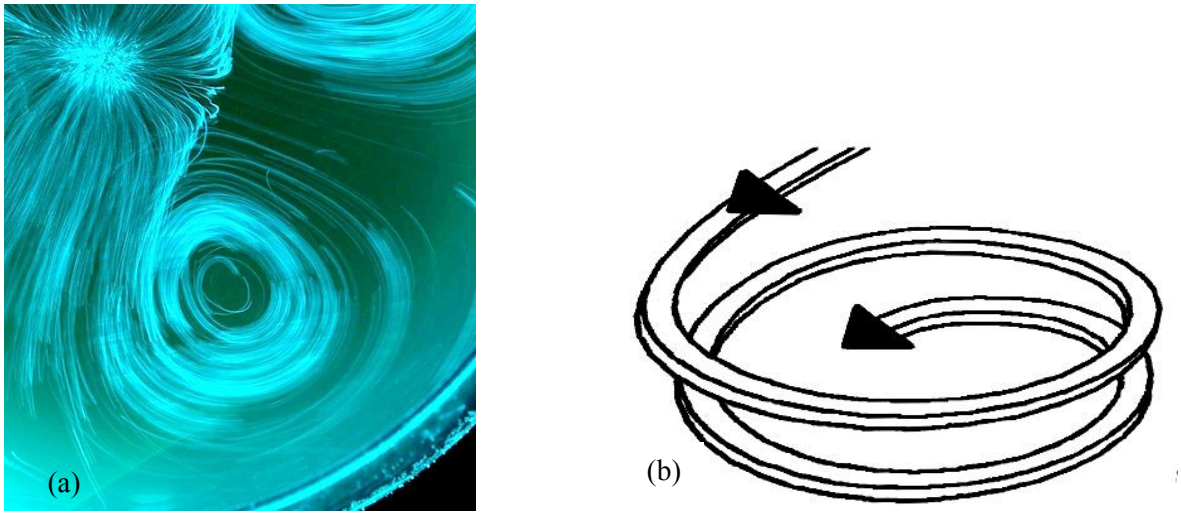

Figure 16: detail of a vortex cell deduced by laser tomography over the free surface of champagne (a) schematic representation of a vortex cell (b).

b) Topological Study

Based on observations, we propose a schematic diagram (Figure 17) of the hydrodynamic processes induced by the bubbles at the origin of vortex flows in a glass of champagne. In this type of flow, bubbles and the surrounding liquid will follow the same path along the z axis of symmetry of the glass (1) toward the surface. This moving liquid will impact the free surface, causing a sudden change of direction. This one is going to inevitably migrate from the center of the glass to the periphery (the edges) (2).

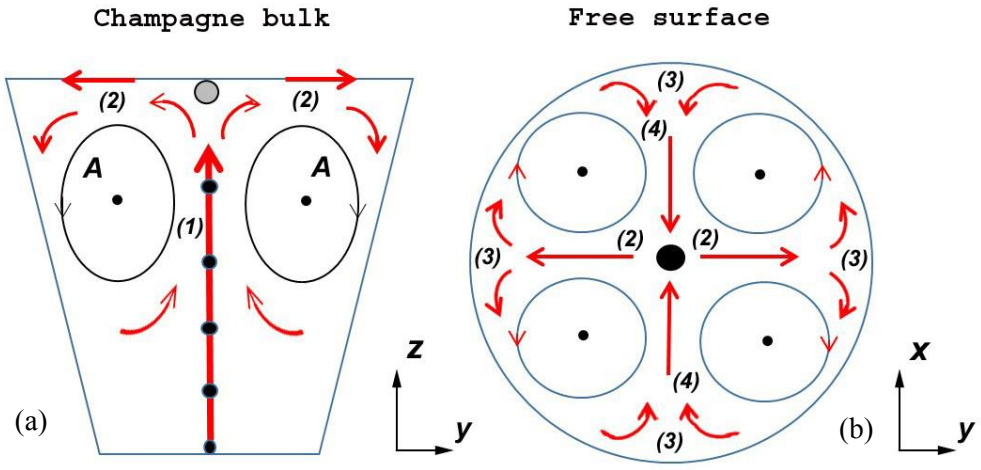

Figure 17: Schematic diagram of the vortical flows of the liquid matrix (a) and corresponding surface streams (b).

When he joined the edge of the glass, the liquid from the surface has not enough energy to dive. However, the movement is powered by the bubbles that bring continuously some liquid to the surface and the liquid, unable to dive back into the periphery, will redirect its way along the glass edge. (3). Inevitably, he will encounter on its path some liquid surface which underwent exactly the same destiny. This event will redirect the flow of liquid from the glass wall to the center and so on (4). Observing the liquid surface (seeded with particles) allowed us to confirm that this liquid dives again in the liquid matrix at the central axis of the glass. Therefore, the surface fluid is organized spontaneously in vortex cells that rotate in opposite directions from each other (just like a gear system). Because there is always flow conservation, the liquid which is found on the surface dives again inexorably continuously feeding the mixing process.

5 Conclusion

Evidence for the presence of ascending bubble driven flow patterns in champagne glasses was done, through laser tomography techniques, under standard tasting conditions. Flow patterns in the champagne bulk were found to strongly differ in size, form and velocity, whether the glass shows natural or artificial effervescence. Moreover, the particle image velocimetry (PIV) technique was used in order to get quantitative data on the velocity fields of flow patterns in laser etched champagne glasses. A topological study help us to understand the flow patterns which have been evidenced through experiments. Spontaneous and self-organized convective cells were also evidenced at the air/champagne interface through classical visualization techniques.

References

[1] Polidori, G., Jeandet, P., Liger-Belair, G., (2009). Bubbles and Flow Patterns in Champagne. American Scientist 97, pp. 294.

[2] Liger-Belair, G., Beaumont, F., Vialatte, M.-A., Jégou, S., Jeandet, P., Polidori, G., (2008). Kinetics and stability of the mixing flow patterns found in champagne glasses as determined by laser tomography techniques: likely impact on champagne tasting. Anal. Chim. Acta 621, pp. 30–37.

[3] Polidori, G., Beaumont, F., Jeandet, P., Liger-Belair, G., (2008). Visualization of swirling flows in champagne glasses. J. Visualization 11, pp. 184.

[4] Beaumont, F., Liger-Belair, .G., and Polidori, G. (2013). Flow patterns in champagne glasses. In AccessScience. McGraw-Hill Education.

[5] Liger-Belair, G., Religieux, J.-B., Fohanno, S., Vialatte, M.-A., Jeandet, P., Polidori, G., (2007). Visualization of Mixing Flow Phenomena in Champagne Glasses under Various Glass-Shape and Engravement Conditions. J. Agric. Food Chem. 55, pp. 882–888.

[6] Polidori, G., Beaumont, F., Jeandet, P., Liger-Belair, G., (2008). Artificial bubble nucleation in engraved champagne glasses. J. Vis 11, pp. 279–279.

[7] Liger-Belair, G., Beaumont, F., Jeandet, P., Polidori, G., (2007). Flow patterns of bubble nucleation sites (called fliers) freely floating in champagne glasses. Langmuir 23, pp. 10976–10983.

[8] Liger-Belair, G., Beaumont, F., Bourget, M., Pron, H., Parvitte, B., Zéninari, V., Polidori, G., Cilindre, C., (2012). Carbon dioxide and ethanol release from champagne glasses, under standard tasting conditions. Adv. Food Nutr. Res. 67, pp. 289–340.

[9] Liger-Belair, G., Villaume, S., Cilindre, C., Polidori, G., Jeandet, (2009). CO_2 volume fluxes outgassing from champagne glasses in tasting conditions:

[10] Perry, A.E., Fairlie B.D. (1974) Critical points in flow patterns, Adv. Geophys. B18, pp 299-315.

[11] Hunt J.C.R. Abell C.J., Peterka J.A. and Woo H., (1978). Kinematical studies of the flows around free or surfaces-mounted obstacles; applying topology to flow visualizations, J. Fluid Mechanics 86, part 1, pp. 179-200.

[12] Perry, A.E., Chong M.S. (1987) A description of eddying motions and flow patterns using critical-point concepts, Annu. Rev. Fluid Mech., 19, pp 125-155.

[13] Perry, A.E., Chong M.S. (1993) Topology of flow patterns in vortex motions and turbulence, Proc. IUTAM Symposium: Eddy structure identification in free turbulent shear flows, Poitiers, Fra., Edited by J.P. Bonnet et M.N. Glauser, Kluwer Academic Publishers, pp. 339-361.

[14] Liger-Belair, G., Beaumont, F., Vialatte, M.-A., Jégou, S., Jeandet, P., Polidori, G., (2008). Kinetics and stability of the mixing flow patterns found in champagne glasses as determined by laser tomography techniques: likely impact on champagne tasting. Anal. Chim. Acta 621, pp. 30–37.

[15] Liger-Belair, G., Religieux, J.-B., Fohanno, S., Vialatte, M.-A., Jeandet, P., Polidori, G., (2007). Visualization of Mixing Flow Phenomena in Champagne Glasses under Various Glass-Shape and Engravement Conditions. J. Agric. Food Chem. 55, pp. 882–888.

[16] Polidori, G., Beaumont, F., Jeandet, P., Liger-Belair, G., (2009). Ring vortex scenario in engraved champagne glasses. J. Visualization 12, pp. 275–282.

[17] Beaumont, F., Popa, C., Liger-Belair, G., Polidori, G., (2012). Revealing ascending bubbble-driven flow patterns in a laser-etched champagne glass by means of particle image velocimetry (PIV). Journal of Flow Visualization and Image Processing 19, pp. 279–289.

[18] Badr, H., Countanceau, M., Dennis, S., Menard, C., (1986). Sur les phénomènes de transposition et de coalescence de tourbillons dans les écoulements décollés. Comptes rendus de l'Académie des sciences. Série 2, Mécanique, Physique, Chimie, Sciences de l'univers, Sciences de la Terre 302, pp. 1127–1130.

[19] Liger-Belair, G., Polidori, G., (2011). Voyage au coeur d'une bulle de champagne. Odile Jacob.

[20] Beaumont, F., Liger-Belair, G., Polidori, G., (2014). Unveiling self-organized convective cells in champagne glasses, Journal of Fluid Structures, in preparation.